JOURNAL OF PROPULSION AND POWER
Vol. 15, No. 2, March–April 1999

Fuel Effects on Lean Blowout and Emissions from a Well-Stirred Reactor

J. W. Blust* and D. R. Ballal†
University of Dayton, Dayton, Ohio 45469-0151
and
G. J. Sturgess‡
Innovative Scientific Solutions, Inc., Dayton, Ohio 45440-3638

The design and development of low-emission, lean premixed aero- and industrial gas-turbine combustors is challenging because of a need to satisfy conflicting requirements of operability, combustion performance, and low emissions. A toroidal well-stirred reactor (WSR) is a laboratory idealization of a compact primary zone of a gas-turbine combustor. Such a WSR was designed, built, and operated at atmospheric pressure to study lean blowout and emissions of CO, unburned hydrocarbons, and NO_x over a range of residence time and fuel–air ratios. A variety of normal and cyclic alkanes, aromatics, and a blend of pure hydrocarbon fuels were tested. Results showed that fuel type affects lean blowout limits, combustion efficiency, and pollutant emissions. These observations have important practical implications to the design of gas-turbine combustors.

Nomenclature

A = Avagadro's number
C = molecular collision factor
(C/H) = carbon to hydrogen mole ratio
E = activation energy
EI = emissions index, g/kg fuel
F = concentration of fuel (percent volume in air)
h = Planck's constant
k = reaction rate
LHV = lower heating value of hydrocarbon, J/kg
LP = loading parameter, g mole/s L atm^n
M = molecular weight of gas mixture
Ma = Mach number at exit to reactor jet
m = mass flow rate, kg/s, or molar flow rate, g mole/s
n = global reaction order
P = pressure
Q = reactor heat loss
R = universal gas constant
T = temperature
t = time
V = reactor volume
x_i = mole fraction of species i
Δs^* = entropy change between states of activated complex and initial reactants
η = efficiency
ρ = density
τ = residence time
ϕ = equivalence ratio

Subscripts
calc = calculated
comb = combustion
eb = eddy breakup
f = flame, fuel
in = inlet
jr = jet ring
min = minimum
o = oxygen
η = Kolmogoroff microscale

Introduction

THE performance requirements of military and civilian aircraft and industrial gas turbines for the next century pose many challenges to designers. The amendments to the 1990 Federal Clean Air Act mandate significant reduction of CO, unburned hydrocarbons (UHC), and NO_x from aero- and land-based gas-turbine engines currently under development. Unfortunately, any solution designed to decrease emissions leads to concurrent penalties in performance, such as poor low-power (idle) efficiency, poor pattern factor, difficult altitude relight, and poor part-load combustion stability. Further, the burning of residual fuels, aromatics, or naphtha in industrial gas-turbine combustors and low-volatility JP-8 fuel in aeroengines makes it imperative to study the effects of fuel type on lean blowout (LBO) and emissions from combustors. A well-stirred reactor (WSR) provides a controlled laboratory combustor configuration to study these effects.

A well-known strategy to reduce NO_x from a gas-turbine engine is to design a lean, premixed, prevaporized (LPP) combustor. Experiments to minimize emission levels in an LPP system have been performed by Anderson,[1] Marek and Papathakos,[2] and Mularz.[3] A well-stirred reactor is simply a laboratory idealization of a gas-turbine combustor. In the present investigation, we have supplied a toroidal WSR with premixed, prevaporized fuel–air mixtures and studied the effects of fuel type on lean blowout, combustion efficiency, and emissions. It should be noted that research using vaporized fuels has been performed in various combustors and reactor configurations.[4–9] Our studies benefit from this previous research work and provide new insights into the effects of fuel type on blowout, efficiency, and emissions.

Presented as Paper 97-2710 at the AIAA/ASME/SAE/ASEE 33rd Joint Propulsion Conference, Seattle, WA, July 6–9, 1997; received Oct. 9, 1997; revision received Nov. 3, 1998; accepted for publication Nov. 3, 1998.

*Ph.D. Student, Department of Mechanical and Aerospace Engineering, 300 College Park; currently Senior Engineer, Combustion Engineering Department, Solar Turbine, Inc., San Diego, CA 92186.
†Professor, Department of Mechanical and Aerospace Engineering, 300 College Park. E-mail: ballal@udri.udayton.edu. Fellow AIAA.
‡Vice President, 2766 Indian Ripple Road. Associate Fellow AIAA.

Experimental Work

WSR Test Facility and Instrumentation

A 250-ml toroidal WSR, as designed by Nenniger et al.[10] and modified by Zelina and Ballal,[11] was used for this experiment. The reactor was constructed of alumina cement, featured a jet ring with 32 stainless-steel jets, each 1-mm i.d., and injected premixed fuel–air mixture at high subsonic velocity (Ma = 0.42–0.85). Figure 1 shows the test facility and instrumentation.

The Horiba emissions analyzers comprised the following units: model MPA-510 oxygen analyzer (0–50 vol %), model FIA-510 total hydrocarbon analyzer (0–10,000 ppm carbon), model VIA-510 CO (0–20 vol %) and CO_2 (0–100 vol %) analyzers, and model CLA-510 SS NO and NO_x analyzers [0–2000 parts per million by volume (ppmV)]. These units were calibrated with gases of the following concentrations: hydrocarbon = 404-ppmV propane, NO = 92 ppmV, NO_2 = 1.6 ppmV, CO = 0.4 vol %, O_2 = 4.03 or 5.02 vol %, and CO_2 = 11.06 vol %. The analyzers used 4 slpm of gas sample with a pressure of ±10 cm of water at ambient. Water was scrubbed from the sample gas to a maximum dew point of 5 C. All emissions are quoted on a dry standard air basis.

A combustion gas sample was drawn from the center of the WSR torus by a water-cooled stainless-steel probe designed by Blust et al.[12] The probe created a pressure drop, and to compensate for it, a pump rated to 12 slpm elevated the sample line pressure. This sample was pumped into each analyzer unit through a heated sampling line. Hydrocarbon speciation at an LBO condition was performed using a gas chromatograph–flame ionization detector (GC–FID, Hewlett–Packard HP 5890A), and the qualitative identification of combustion products was performed by comparing retention times of unknown analytes to those of pure compounds.

Combustion temperature, T_f, was measured by inserting a type B thermocouple (platinum-6% rhodium, platinum-30% rhodium) into the torus. This thermocouple was coated with alumina ceramic to protect the thermocouple from the reactor environment. All thermocouples were calibrated, and temperature measurements were corrected for heat loss by conduction and radiation and heat gain by convection and catalysis as described by Blust.[13] Figure 2 shows the close agreement obtained between temperatures measured using two different methods. Such a procedure ensured the accuracy of combustion temperature measurements.

A vaporizer was built to evaporate liquid fuels, mix the vaporized fuel with air, and then supply this combustible mixture to the WSR. The vaporizer used a 3-kW air heater (Hotwatt), pressurized fuel tank, vaporization chamber, various flow meters, nozzle air line, safety devices, and a fuel atomization nozzle. Heated air was injected to establish a recirculation zone in the vaporizer. This recirculation provided a residence time as high as 1.2 s to fully vaporize the liquid fuel (Ballal and Lefebvre[14] have estimated a vaporization time of 0.36 s for *n*-

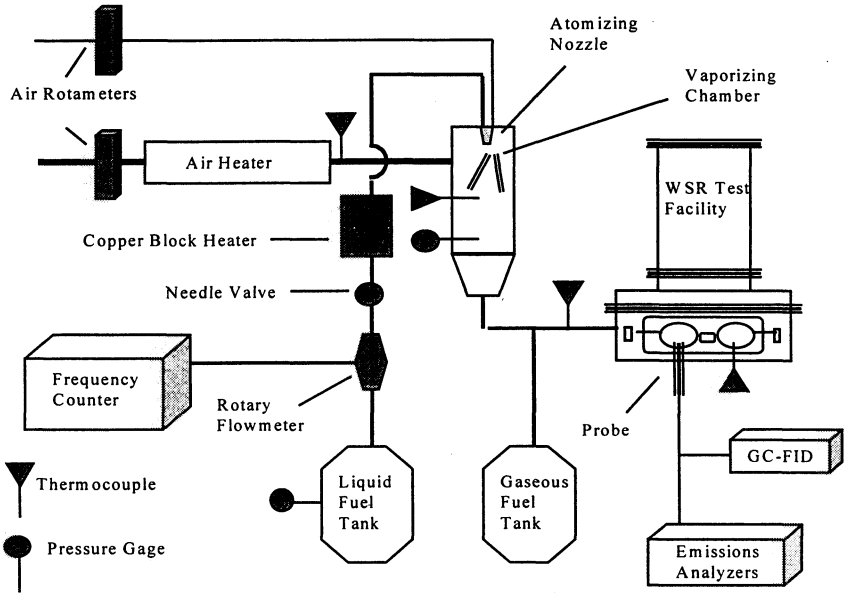

Fig. 1 WSR test facility and associated instrumentation.

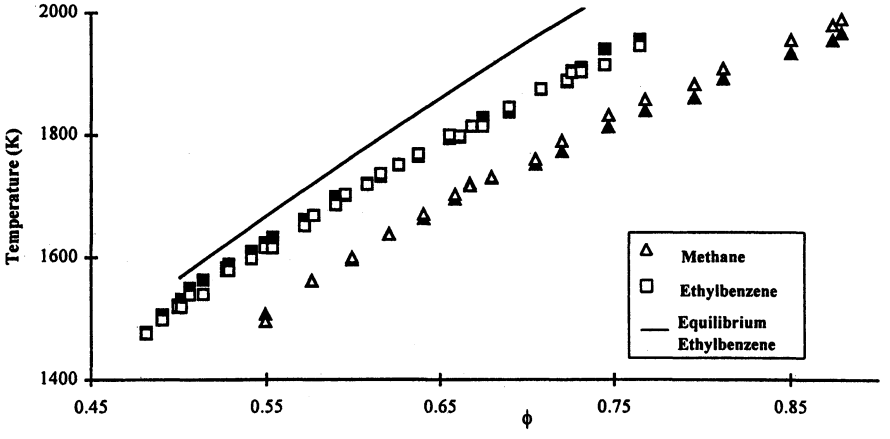

Fig. 2 Reaction temperature vs equivalence ratio at 7.3 ms residence time. Solid, thermocouple; hollow, calorimeter; and ——, Gordon and McBride[21].

Table 1 WSR test matrix

Hydrocarbon	CN	(C/H)	τ, ms	ϕ_{min}	ϕ_{max}	T_{fmin}, K	T_{fmax}, K
Methane	1	0.25	7.3	0.55	0.88	1507	1967
			6.32	0.59	0.83	1517	1918
Ethane	2	0.333	7.26	0.48	0.84	1407	1996
Cyclohexane	6	0.5	7.47	0.48	0.82	1429	1981
			5.22	0.51	0.78	1536	1922
n-heptane	7	0.4375	7.19	0.53	0.84	1517	1975
			5.49	0.54	0.81	1595	1974
Toluene	7	0.875	7.32	0.46	0.79	1499	1946
			5.35	0.5	0.78	1552	1936
Ethylbenzene	8	0.8	7.43	0.48	0.76	1478	1958
			5.33	0.49	0.67	1546	1839
Cracked fuel simulant	2.52	0.5081	6.75	0.49	0.77	1530	2007
			5.17	0.46	0.76	1391	1969
n-dodecane	12	0.4615	7.39	0.46	0.8	1357	1979
			5.2	0.55	0.79	1581	1983

heptane). Nominal reactor residence time, τ, was computed by $\tau = PV/(RT_f m/M)$.

The WSR was operated over the range of equivalence ratios ϕ = 0.43–0.88, loading parameter[15] LP ~ 1.3 g mol/s L atm$^{1.75}$, residence times $\tau \sim 5$–8 ms, and reactor temperatures T_f = 1350–2000 K. Fuels studied in the WSR were: methane, ethane, cyclohexane, *n*-heptane, *n*-dodecane, toluene, ethylbenzene, and a cracked fuel simulant comprising 15% methane, 25% ethane, and 60% ethylene by volume.

Error Analysis

Gaseous fuel flow was monitored to within ±2% of reading using a Gilmont rotameter, and air flow was monitored to within ±2% of full scale using a Brooks rotameter. The combined error produced an uncertainty of ±3.5% in ϕ during the combustion of methane in air. Nozzle air was monitored to within ±2% of full scale using a Gilmont rotameter. Liquid hydrocarbons were controlled to within ±0.3 g/min by the liquid fuel delivery system. The combined error produced an uncertainty of ±3.5% in ϕ during combustion of a liquid fuel in air. The measurement of combustion temperature T_f was repeatable to within ±30 K. The Horiba emissions analyzers have an accuracy to within 1% of full scale. This represented an error of 2-ppmV NO_x, 50-ppmV CO, 10-ppmV carbon for UHC, 0.25 vol % O_2, and 0.5 vol % CO_2. Residence time was typically controllable to within ±0.6 ms. Additionally, CO measurements were repeatable from day-to-day within ±100 ppmV, and NO_x within ±1.5 ppmV. UHC measurements close to lean blowout suffered from poor repeatability. The preceding uncertainties in temperature and emissions translate into uncertainty in ϕ_{LBO} of ±0.02. Finally, Blust et al.[12] demonstrated minimum oxidation reactions in the water-cooled stainless-steel probe.

Test Conditions

Table 1 shows matrix of tests performed at atmospheric pressure. A volumetric mix of 13% CH_4, 22% C_2H_6, 52% C_2H_4, 13% C_7H_8 by volume produced a fuel with carbon number (CN) = 2.52 and carbon to hydrogen mole ratio, (*C/H*) = 0.5081. This fuel was selected as a simulant for heavy, aromatic-containing fuels that are cracked using thermal or catalytic processes into light fractions with residual light aromatics.

Well-Stirred Condition

To obtain unambiguous results, the WSR must be both micromixed and macromixed. For micromixing, the Kolmogoroff microscale time of the combustion gas, t_η, must be less than the chemical reaction time of the process. Now, a typical value of Kolmogoroff microscale time in the reactor was t_η = 19 μs, as calculated by Zelina and Ballal,[16] using the turbulent flow theory. For methane–air combustion at τ = 6.0 ms, T_f = 1747 K, ϕ = 0.7, P = 1 atm, chemical reaction time was = 25 μs, CO oxidation time = 500 μs, and NO_X formation time = 20 μs as calculated by Getz[17] using the Miller and Bowman[18] mechanism and perfectly stirred reactor (PSR) code,[19] with CHEMKIN-II formalism.[20] This analysis suggests that the WSR was sufficiently well mixed at the microscale level.

Successful macromixing necessitates the WSR having the proper residence time distribution (RTD) and spatial homogeneity of species and temperature. In an earlier investigation, Zelina and Ballal[16] verified the RTD and demonstrated the spatial homogeneity of the WSR. Maximum detected variabilities were found to be T_f = ±25 K, NO_X = ±2.5 ppmV, and CO = ±90 ppmV. These tests suggested that the WSR was successfully macromixed.

Results and Discussion

Flame Temperature Measurement

Figure 2 shows a plot of measured T_f against ϕ for the combustion of methane and ethylbenzene fuels at τ = 7.3 ms. Also plotted is the calculated equilibrium flame temperature vs ϕ for ethylbenzene using the Gordon and McBride[21] code. It is observed that the measured temperature is always lower than the corresponding equilibrium flame temperature because of heat loss and also because of a finite reactor residence time. Also, the thermocouples measure flame temperatures that are in close agreement with calorimeter measurements.

LBO Measurement

Figure 3 shows a plot of LBO equivalence ratio vs WSR loading parameter for several hydrocarbons. The LBO condition was characterized by a rapid, large temperature drop, and preceded by a substantial increase in UHC and noise leading to complete extinction. Also, at the threshold of extinction, we measured T_f, ϕ, reactant flow rates, and the emission index (EI) of CO and UHC. Finally, the static flammability limits (for LP = 0) of these fuels as quoted by Lewis and Von Elbe[22] are also included here. These results can be explained by the WSR stability theory.

Briefly, the rate of fuel and air reaction is expressed by the material balance equation:

$$\eta_{comb}\phi m = \mathrm{CVT}_f^{1/2}\exp(-E/RT_f)\rho^n x_f^r x_o^{n-r} \qquad (1)$$

where m is the molar flow rate of reactants; ρ is the density of reactants; E is activation energy; x_i is the mole fraction of fuel, *f*, or oxygen, *o*; and the global reaction order of methane and ethane is n = 1.75 (Lefebvre[23]), and $r = n - 1$. Now, from Kanury,[24] the molecular collision factor C may be calculated as

$$C = \frac{RT_f^{1/2}}{hA}\exp\left(\frac{\Delta s^*}{R}\right) \qquad (2)$$

For lean mixtures, Eq. (1) may be rewritten to yield LP or E as

$$\mathrm{LP} = \frac{m}{VP^n} = \exp\left(\frac{-E}{RT_f}\right)\frac{Cx_f^{0.75}x_o}{T_f^{1.25}\eta_{\mathrm{comb}}\phi(R/M)^{1.75}} \quad (3)$$

$$\mathrm{E} = RT_f\,\ell n\left[\frac{Cx_f^{0.75}x_o}{LP\cdot T_f^{1.25}\eta_{\mathrm{comb}}\phi(R/M)^{1.75}}\right] \quad (4)$$

In Eq. (2), the entropy of the activated complex was found by applying a quantity of energy equal to E to the energy of reactants and evaluating entropy at this condition. Next, an iterative calculation provides values of C and E; for methane E = 52 kcal/mol and $C = 9.4 \times 10^{14}$ $K^{-1/2}$ s^{-1} m^{3n-3} mol^{1-n}, and for ethane E = 49 kcal/mol and $C = 1.3 \times 10^{15}$ $K^{-1/2}$ s^{-1} m^{3n-3} mol^{1-n}. Substitution of these values in Eq. (3) together with the measured values of other parameters (LBO, T_f, and η_{comb}) provides a relationship between LP vs ϕ that is shown plotted in Fig. 3. It is observed that the predictions are in good agreement with the measurements.

Combustion Efficiency Measurement

Figure 4 shows the combustion efficiency η_{comb} plotted against CN for several fuels at LP = 1.3 g mol/s L atm^n. The combustion efficiency was calculated from the measured values of emissions indices of CO and UHC using the Aerospace Recommended Practice (ARP 1533[25]) relationship:

$$\eta_{\mathrm{comb}} = 1 - (10109EI_{\mathrm{co}}/\mathrm{LHV}) - (EI_{\mathrm{UHC}}/1000) \quad (5)$$

The results clearly demonstrate that, in general, as CN increases, η_{comb} decreases gradually from 99 to 94%, i.e., fuel type affects combustion efficiency. These results were found to be relatively independent of ϕ or T_f within the uncertainty limits of these experiments. To test the sensitivity of measured η_{comb} to UHC and CO species, two curves of η_{comb}, one taking into account only CO, the other only UHC species, are also plotted in Fig. 4. The curve of η_{comb} with only UHC shows that, for CN < 7, η_{comb} was constant for all fuels and slightly decreased for toluene and n-dodecane. The curve of η_{comb} with only CO shows that methane has the highest combustion efficiency. Thus, decreasing η_{comb} at higher CN was attributable to incomplete combustion of UHC products for most fuels.

It should be noted that the LBO combustion efficiencies in these WSR experiments are higher than those found in practical gas-turbine combustors. This is because of a high degree of uniform mixing in a WSR and the use of single as opposed to multicomponent (wide-cut) hydrocarbon fuels studied herein. The LBO limit of a gas-turbine combustor is wider than that of a WSR because incomplete mixing in the former produces pockets of locally flammable (usually lighter fuel components) mixture that sustains combustion. However, this combustion process also produces a large amount of CO and UHC, thereby lowering the combustion efficiency. For example, Fig. 4 shows that η_{comb} is lower for a cracked fuel simulant (CN = 2.52) than for pure fuels such as ethane or cyclohexane.

CO_2 and O_2 Measurements

In a WSR operating in the stable mode, CO_2 concentration should peak and oxygen concentration should drop to near-zero at stoichiometric equivalence ratios. Figure 5 shows typical measured CO_2 and O_2 concentrations (vol %) and calculated equilibrium values as a function of equivalence ratio. As expected, CO_2 increased and O_2 decreased as ϕ approached unity. Also, there is excellent correlation between predictions and measurements that demonstrates a close to ideal behavior of the WSR.

CO and UHC Measurements

The CO and UHC emissions are important because they represent a direct measure of combustion inefficiency. If the

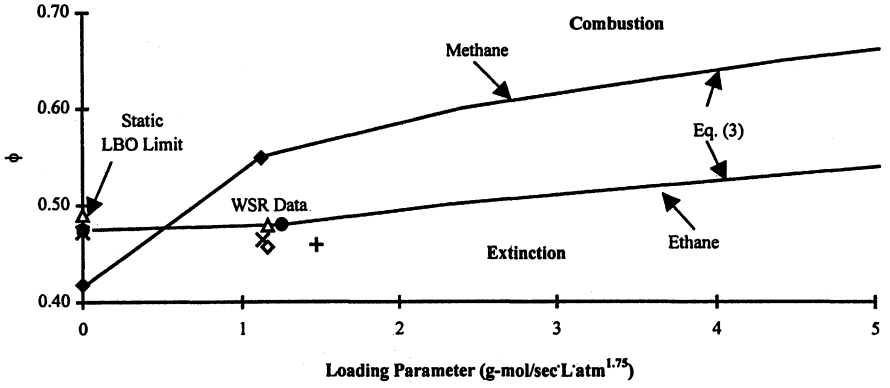

Fig. 3 LBO equivalence ratio vs loading parameter for several fuels: ♦, methane; ●, ethane; △, cyclohexane; ◇, n-dodecane; ×, toluene; +, cracked fuel simulant; and ——, Eq. (3).

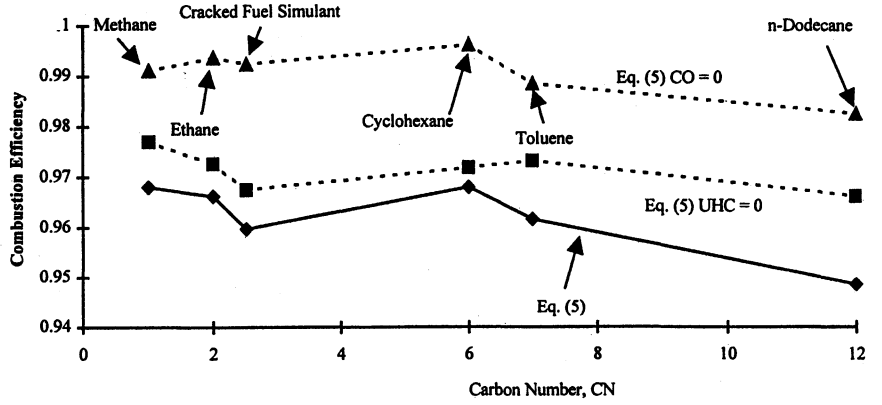

Fig. 4 Combustion efficiency [Eq. (5)] vs CN for several fuels. Also, the two curves (– – –) show the relative effects of CO and UHC on combustion efficiency.

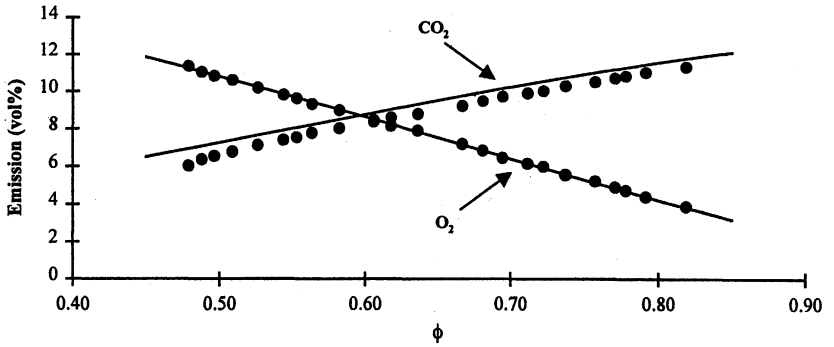

Fig. 5 CO_2 and O_2 concentration vs equivalence ratio for cyclohexane at residence time 7.5 ms. ——, equilibrium calculations using Gordon and McBride[21] code.

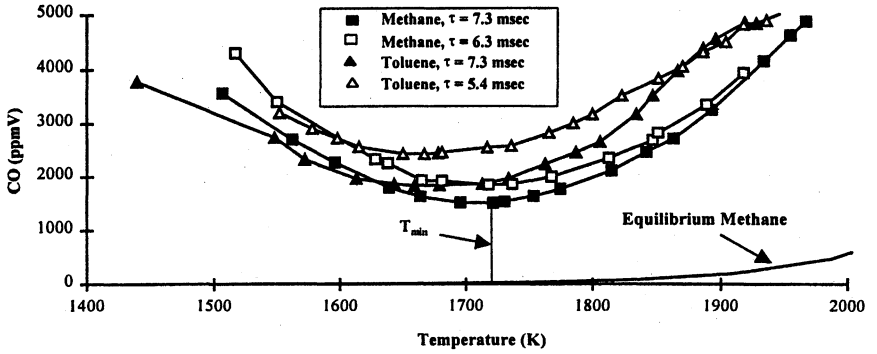

Fig. 6 CO emissions vs reaction temperature. Temperature at minimum CO emission and equilibrium methane calculation are shown (Gordon and McBride[21]).

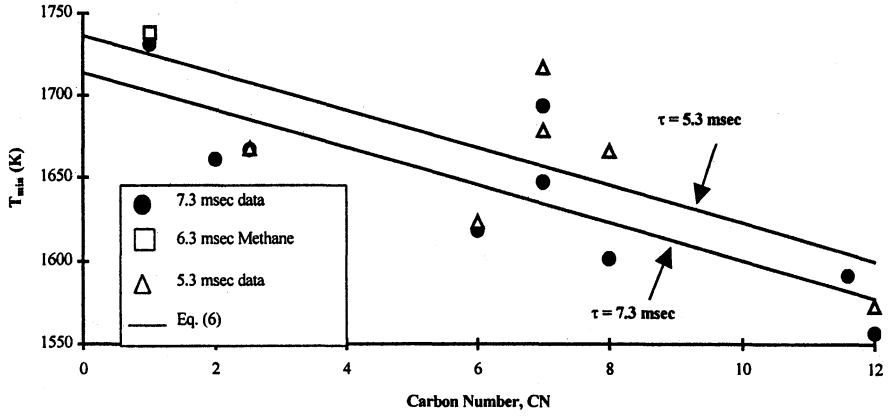

Fig. 7 Temperature at minimum CO emission vs CN. Also predictions using Eq. (6) are shown.

combustor operates fuel-rich, has inadequate mixing, or is quenched by cold air, large quantities of CO (which is relatively resistant to oxidation), will be emitted as a result of the lack of oxygen needed to complete the reaction to CO_2, or insufficient residence time provided for CO to be oxidized. UHC emissions are associated with poor atomization, inadequate burning rates, insufficient residence time, and premature quenching.

Figure 6 shows profiles of CO (ppmV) vs T_f from methane and toluene fuels at residence times of 7.3, 6.3, and 5.4 ms. In general, all hydrocarbons exhibited a U-shaped trend in CO concentration. As temperature increased, CO concentration first decreased as reaction rate of CO consumption increased, next a minimum was reached, and finally, the CO concentration increased as a result of an increased rate of CO_2 dissociation. Also, it is observed that decreasing residence time increased CO, and these CO concentrations are significantly higher than, for example, the computed equilibrium CO concentration (assuming infinite residence time) for methane.

Figure 7 shows plots of temperature, T_{min} at which CO minima occurs vs carbon number CN at 7.3 and 5.3 ms residence times (methane τ = 7.3 or 6.3 ms), corrected to the standard inlet temperature 296 K by using $T_{min} = T_f - (T_{in} - 296)$ K. These results show that as the carbon number of the fuel is increased, T_{min} decreases. This rule applied to alkanes and aromatics, with the cracked fuel simulant classified as an alkane. Also, the effect of decreasing residence time was to increase T_{min} presumably, because of a reduction of CO oxidation at short residence time, whereas the CO_2 dissociation rate proceeded quickly regardless of residence time. All of the data plotted in Fig. 7 can be approximated by a relationship:

$$T_{min} = -11.35\text{CN} - 11.27\tau(\text{ms}) + 1796 \qquad (6)$$

Figure 8 shows emissions index of CO from several hydrocarbons, at several values of T_f, plotted as a function of CN at a residence time of 7.3 ms; cracked fuel simulant is treated as an alkane. As shown, alkanes, sans methane, displayed a slight increase in CO as CN increased. Methane produced more CO than any other fuel, presumably because the stable methane molecule resists quick oxidation. In contrast to alkanes, the two aromatic fuels showed a decrease in CO as CN increased from 7 to 8. The primary path of toluene consumption at high temperature is C–C rupture, resulting in $C_7H_8 \rightarrow C_6H_5 + CH_3$. The C–H rupture of the methyl chain occurs quickly, but the $C_7H_7 + H$ reaction is rapidly equilibrated, and as suggested by Lindstedt and Maurice,[26] toluene is recycled. Because of this recycling, toluene is resistant to oxidation, resulting in considerable UHC and CO in the products.

Figure 9 shows the emissions indices of UHC from several hydrocarbons at several T_f, plotted as a function of CN at residence time of 7.3 ms. As shown, alkanes showed a rapid decrease, then a modest increase in UHC as CN increased. The high UHC for methane at 1500 K is a result of the WSR operation at LBO. Ethane behaved more like other alkanes. Toluene produced more UHC at a given temperature than other hydrocarbons besides methane, whereas ethylbenzene produced a quantity of UHC more akin to alkanes of the same CN. As with CO, similarity between methane and ethane, toluene and ethylbenzene is observed.

Table 2 summarizes the composition of UHC at LBO from several hydrocarbons. Ethylene is the most abundant intermediate hydrocarbon product from *n*-heptane, and the mechanisms for combustion of other alkanes are similar. Thus, ethylene is the major component of UHC from lean alkane combustion. Conversely, acetylene was the most abundant UHC component from toluene because it is a product of the decomposition of benzene, which itself is a common product of the decomposition of toluene. As a result, trace amounts of C6 were also identified in the UHC mixture from toluene. The cracked fuel simulant behaved more like an alkane than an aromatic.

NO_x Measurements

NO_x emission from gas-turbine combustors is typically associated with primary zone combustion at near-stoichiometric conditions and high-power settings. To reduce NO_x, advanced combustor designs employ uniform/pre mixing, fuel-lean com-

Table 2 Effluent hydrocarbon species by volume percent of UHC

Hydrocarbon	CH_4	C_2H_4	C_2H_6	C_2H_2	C_3H_6	C4	C5	C6	τ, ms	ϕ	T_f, K
Toluene	27	14.5	0	55.5	0	0	0	3	7.56	0.46	1439
Cyclohexane	30	49	12	9	0	0	0	0	6.83	0.51	1513
Ethane	20	40	40	0	0	0	0	0	6.95	0.48	1407
Cracked fuel simulant	23	58	16	3	0	0	0	0	5.96	0.46	1391
n-dodecane	19	60	6	2	6	3	2	2	7.71	0.46	1357

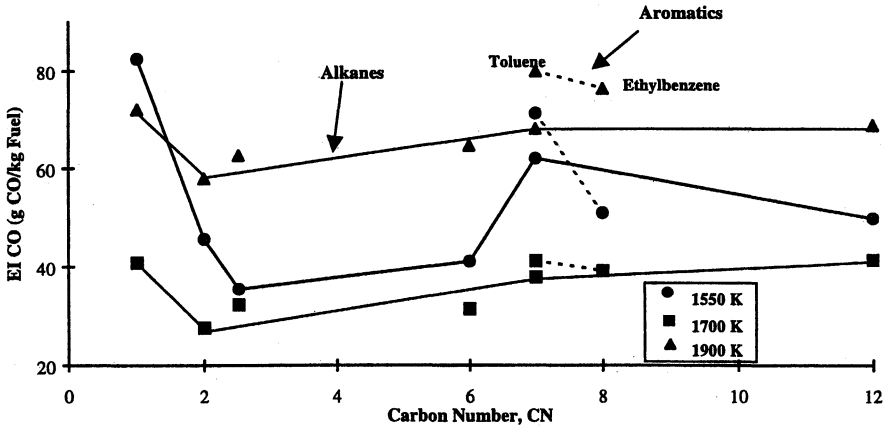

Fig. 8 Emissions index of CO vs CN for several fuels at a nominal residence time of 7.3 ms.

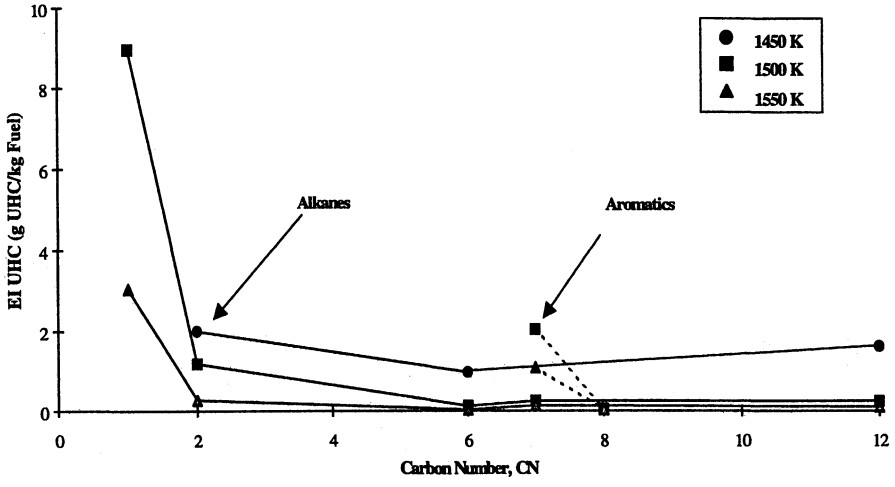

Fig. 9 Emissions indices of UHC vs CN for several fuels at a nominal residence time of 7.3 ms.

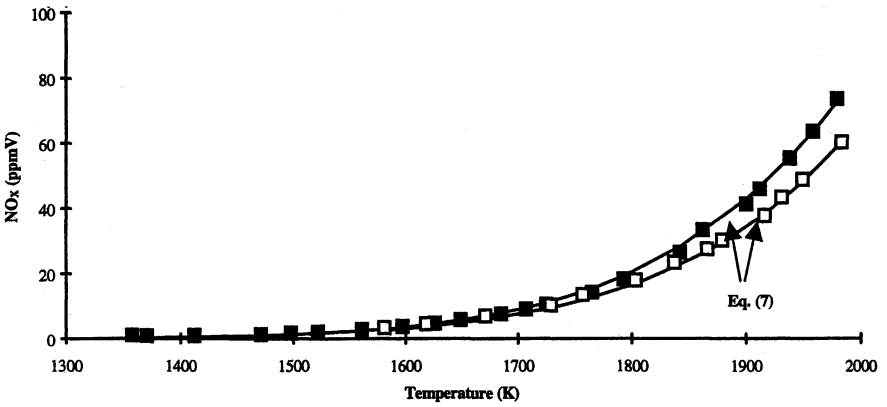

Fig. 10 NO_X emissions vs reaction temperature for *n*-dodecane (square) at residence time 7.3 ms (solid symbol) and 5.3 ms (hollow symbol). ——, predictions for *n*-dodecane using Eq. (7).

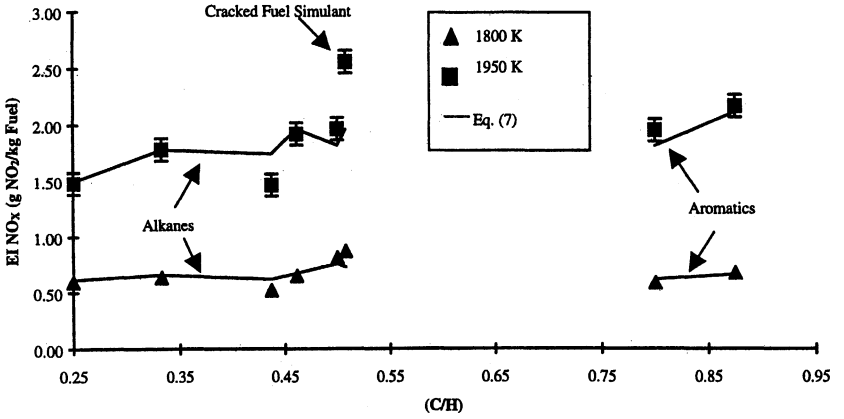

Fig. 11 Emissions indices of NO_X vs (C/H) ratio of fuels at a nominal residence time of 7.3 ms.

bustion, and/or even water/steam injection to decrease reaction temperature. The formation of species such as NO and NO_2 is a complex function of temperature, residence time, equivalence ratio, and detailed chemical kinetics. Recently, Capehart et al.[6] and Nicol et al.[27] discussed fuel nitrogen mechanisms, the thermal NO (Zeldovich) mechanism, super-equilibrium effects, prompt NO mechanism, and N_2O mechanism. Figure 10 shows profiles of NO_X (ppmV) vs T_f from *n*-dodecane. As equivalence ratio (and hence, also reaction temperature) increased above its LBO value, NO_X emissions increased gradually, then rapidly for $T_f > 1800$ K, because of the extended Zeldovich NO_X mechanism. Also, increasing residence time increased NO_X. The present work suggests the following equation for *n*-dodecane:

$$NO_X = k\tau^{1/2} \exp(-E/RT_f) \text{ (ppmV)} \qquad (7)$$

where k = 9,229,000 ppmV $NO_X/ms^{1/2}$, and E = 50,240 kcal/g mol. Equation (7) was plotted in Fig. 10 and yields a satisfactory prediction of experimental results in the range of residence time 5–8 ms. The relationship, $NO_X \propto \tau^{1/2}$ was also observed for other fuels such as methane, *n*-heptane, cracked fuel simulant, toluene, and ethylbenzene. This effect of residence time implies that the rate of change of formation $d(NO_X)/dt \propto \tau^{-1/2}$, i.e., formation rate is greater at shorter residence time.

Because all tested fuels exhibited $NO_X \propto \tau^{1/2}$ trend, values of E and k were calculated for all fuels using the iterative procedure described by Nicol et al.[27] A range of these calculated results over (C/H) ratio of 0.25–0.9 were E = 52–71 kcal/g mol and k = 11–922 K ppmV $NO_X/1000$ $ms^{1/2}$. These results suggest that NO_X increases with an increase in the (C/H) ratio because of the propensity of the hydrocarbon to produce CH_X radicals. The calculated values of E and k together with other test parameters were substituted in Eq. (7) and predictions of emissions index EI_{NO_X} were obtained. For the EI NO_X calculations, all NO_X was treated as NO_2.

Figure 11 shows measured and calculated emissions indices of NO_X vs (C/H) ratio of the various fuels tested. These measurements were made at a nominal residence time of 7.3 ms and at T_f = 1800 K and 1950 K, with alkanes and aromatics plotted separately, and with cracked fuel simulant plotted with the alkanes. A gradual increase in NO_X emissions is observed as (C/H) ratio is increased from 0.25 (methane) to 0.875 (toluene). Further, this increase is even more pronounced at a higher temperature, T_f = 1950 K. Also, the two aromatic fuels showed a similar increase in NO_X with (C/H) ratio, with toluene producing more NO_X than ethylbenzene. Finally, the NO_X calculations accurately predict increase in NO_X as (C/H) ratio is increased. Lindstedt and Maurice[26] suggested that branched aromatic molecules at high temperature (>1850 K) form a greater quantity of prompt NO_X precursor such as CH_X than alkanes do. Presumably, this mechanism increases prompt NO_X formation, and hence, also the total NO_X. These observations suggest an increase in pollutant emissions from gas turbines burning crude or residual fuels with high (C/H) ratio.

Conclusions

A toroidal WSR, which represents a laboratory idealization of a primary zone of a gas-turbine combustor, was used to study lean blowout, combustion efficiency, and gaseous emissions from several fuels. The following conclusions resulted from this research.

1) All fuels, except methane, showed a lean blowout limit at ϕ = 0.47 with LP = 1.3 g mol/s L $atm^{1.75}$ (methane LBO was ϕ = 0.55). These measurements and combustion stability theory yielded global activation energies and collision factors for many fuels; e.g., E = 52 kcal/mol and $C = 9.4 \times 10^{14}$ $K^{-1/2}$

s^{-1} m^{3n-3} mol^{1-n} for methane, and E = 49 kcal/mol and C = 1.3×10^{15} $K^{-1/2}$ s^{-1} m^{3n-3} mol^{1-n} for ethane.

2) Combustion efficiency η_{comb} decreased as fuel CN increased. This relation was observed for alkanes, aromatics, and cracked fuel simulant.

3) Both fuel type (alkanes, aromatics, etc.) and CN affect CO emissions at the same temperature and residence time. In general, alkanes produced more CO as CN increased (except methane), and toluene produced more CO than ethylbenzene. Also, increasing residence time decreased CO emissions. Finally, Eq. (6) provides a relationship between the reaction temperature at which CO emission approaches a minimum vs the CN of the fuel.

4) UHC emissions from alkanes decreased greatly from methane to ethane and remained unchanged for higher CN fuels. Toluene produced more UHC emissions than alkanes at the same temperature. At a low reaction temperature ($T_f < 1600$ K), increasing residence time decreased UHC emissions.

5) Fuel type (C/H ratio) influenced NO_x emissions. As (C/H) ratio increased, NO_x increased, for both alkanes and aromatics. Increasing residence time increased NO_x emissions. Equation (7) provided a good prediction of NO_x emissions in the range of residence times of 5–8 ms.

Acknowledgments

This work was supported by the U.S. Air Force Wright Laboratory, Aero Propulsion and Power Directorate, Wright–Patterson Air Force Base, Ohio, under Contract F33615-92-C-2207, with Charles W. Frayne serving as the Technical Monitor. The authors are grateful to Rich Striebich and Matthew Getz for providing technical assistance.

References

[1]Anderson, D. N., "Effects of Equivalence Ratio and Dwell Time on Exhaust Emissions from an Experimental Premixing Prevaporizing Burner," American Society of Mechanical Engineers, Paper 75-GT-69, June 1975.

[2]Marek, C. J., and Papathakos, L. C., "Exhaust Emissions from a Premixing, Prevaporizing Flame Tube Using Liquid Jet A Fuel," NASA TM X-3383, April 1976.

[3]Mularz, E. J., "Lean, Premixed, Prevaporized Combustion for Aircraft Gas Turbine Engines," NASA TM-79148, June 1979.

[4]Sturgess, G. J., "Assessment of an Abbreviated Jet A/JP-5/JP-8 Reaction Mechanism for Modeling Gas Turbine Engine Gaseous Emissions," AIAA Paper 97-2709, July 1997.

[5]Brezinsky, K., Litzinger, T. A., and Glassman, I., "The High Temperature Oxidation of the Methyl Side Chain of Toluene," *International Journal of Chemical Kinetics*, Vol. 16, 1984, pp. 1053–1074.

[6]Capehart, S. A., Lee, J. C. Y., Williams, J. T., and Malte, P. C., "Effect of Fuel Composition on NO_x Formation in Lean Premixed Prevaporized Combustion," American Society of Mechanical Engineers, Paper 97-GT-336, June 1997.

[7]Dagaut, P., Reuillon, M., and Cathonnet, M., "Experimental Study of the Oxidation of *n*-Heptane in a Jet Stirred Reactor from Low to High Temperature and Pressures up to 40 Atm," *Combustion and Flame*, Vol. 101, 1995, pp. 132–140.

[8]Vaughn, C. B., Howard, J. B., and Longwell, J. P., "Benzene Destruction in Fuel Rich Jet-Stirred Combustion," *Combustion and Flame*, Vol. 87, 1991, pp. 278–288.

[9]Zelina, J., Blust, J. W., and Ballal, D. R., "Combustion of Liquid Fuels in the Well Stirred Reactor," American Society of Mechanical Engineers, Paper 96-GT-047, June 1996.

[10]Nenniger, J. E., Kridiotis, A. C., Chomiak, J., Longwell, J. P., and Sarofim, A. F., "Characterization of a Toroidal Well-Stirred Reactor," *20th Symposium (International) on Combustion*, The Combustion Inst., Pittsburgh, PA, 1984, pp. 473–479.

[11]Zelina, J., and Ballal, D. R., "Combustion Studies in a Well Stirred Reactor," AIAA Paper 94-0114, Jan. 1994.

[12]Blust, J. W., Getz, M. G., and Zabarnick, S., "Probe Design Optimization for the Well Stirred Reactor," AIAA Paper 97-0907, Jan. 1997.

[13]Blust, J. W., "Effects of Fuel Structure on Emissions and Stability in the Well Stirred Reactor," Ph.D. Dissertation, Univ. of Dayton, Dayton, OH, 1998.

[14]Ballal, D. R., and Lefebvre, A. H., "Ignition and Flame Quenching of Flowing Heterogeneous Fuel-Air Mixtures," *Combustion and Flame*, Vol. 35, 1979, pp. 155–168.

[15]Longwell, J. P., and Weiss, M. A., "High Temperature Reaction Rates in Hydrocarbon Combustion," *Industrial and Engineering Chemistry*, Vol. 47, 1955.

[16]Zelina, J., and Ballal, D. R., "Emissions Studies in a Well-Stirred Reactor and Applications to Combustion Modeling," *Proceedings of FACT*, Vol. 21, American Society of Mechanical Engineers, New York, 1996, pp. 255–263.

[17]Getz, M. G., "Investigation of Halon 1301 Interactions in Methane Combustion," M.S. Thesis, Univ. of Dayton, Dayton, OH, 1997.

[18]Miller, J. A., and Bowman, C. T., "Mechanism and Modeling of Nitrogen Chemistry in Combustion," *Progress in Energy and Combustion Science*, Vol, 15, No. 3, 1989, pp. 287–338.

[19]Glarborg, P., Kee, R. J., Grcar, J. F., and Miller, J. A., "PSR: A Fortran Program for Modeling Well-Stirred Reactors," Sandia National Lab., SAND86-8209 UC-4, Livermore, CA, 1988.

[20]Kee, R. J., Miller, J. A., and Jefferson, T. H., "CHEMKIN: A General-Purpose, Problem-Independent, Transportable, FORTRAN Chemical Kinetics Code Package," Sandia National Lab., SAND80-8003, Livermore, CA, 1980.

[21]Gordon S., and McBride, B. J., "Computer Program for Calculation of Complex Chemical Equilibrium Compositions, Rocket Performance, Incident and Reflected Shocks, and Chapman-Jouget Detonations," NASA, SP-273 Interim Revision, 1976.

[22]Lewis, B., and Von Elbe, G., *Combustion, Flames and Explosions of Gases*, 2nd ed., Academic, New York, 1961.

[23]Lefebvre, A. H., *Gas Turbine Combustion*, Hemisphere, New York, 1983.

[24]Kanury, A. M., *Introduction to Combustion Phenomena*, Vol. 2, Gordon and Breach, New York, 1984, pp. 30–42.

[25]Anon., *Procedure for the Calculation of Gaseous Emissions from Aircraft Turbine Engines*, Aerospace Recommended Practice 1533, Society of Automotive Engineers, Warrendale, PA, 1994, pp. 1–36.

[26]Lindstedt, R. P., and Maurice, L. Q., "Detailed Kinetic Modeling of Toluene Combustion," *Combustion Science and Technology*, Vol. 120, No. 2, 1996, pp. 119–167.

[27]Nicol, D. G., Steele, R. C., Marinov, N. M., and Malte, P. C., "The Importance of the Nitrous Oxide Pathway to NO_x in Lean-Premixed Combustion," *Journal of Engineering for Gas Turbines and Power*, Vol. 117, No. 1, 1995, pp. 100–111.